1994

Acoustical Holography in Spherical Coordinates for Noise Source Identification

L. A. DeVries
Purdue University

J. S. Bolton
Purdue University

ACOUSTICAL HOLOGRAPHY IN SPHERICAL COORDINATES FOR NOISE SOURCE IDENTIFICATION

L.A. DeVries and J.S. Bolton

Ray W. Herrick Laboratories, School of Mechanical Engineering
Purdue University
West Lafayette, IN 47907-1077

ABSTRACT

During a study of reciprocating refrigerator compressor noise, it was desired to develop a new technique for visualizing of the vibrations of the shell surface. Previous investigators have shown the value of acoustical holography for this purpose in other applications. However, the spherical geometry of the compressor of interest required the use holography in spherical coordinates. The present work involved checking the accuracy of acoustical holography in spherical coordinates through numerical simulations, and applying the technique to experimental cases including a shell driven by a shaker and the actual compressor in operation on a test stand.

INTRODUCTION

Acoustical holography for the purpose of noise source identification has most often been applied in planar geometries, as summarized by Maynard et al [1]. However, many small machines have shapes that make planar holography inconvenient. In these cases, spherical or cylindrical analysis geometries may yield better results. Several investigators have developed holographic algorithms incorporating solutions of the wave equation in cylindrical and spherical coordinates. For spherical geometries the technique has been applied in cases where the sound source may be entirely enclosed by a sphere on which sound pressure is measured. Weinreich and Arnold [2] have described a method in which a boom system was employed to measure the complex sound pressure on two concentric spheres. They then expanded the solution of the wave equation in spherical coordinates in terms of the spherical harmonics whose amplitudes were determined from the measured pressures; their method can be used to characterize the sound field when both incoming and outgoing waves are present. Laville et al. [3] have developed a technique based on the assumption that the sound field comprises outgoing waves only, and which allows the complex pressure to be expressed as a function of sound intensity and the mean square pressure measured on a single spherical surface. The present work was conducted in order both to confirm the accuracy of spherical holography in simulation, and to extend its application to noise source identification for small machines, specifically a refrigeration compressor. As employed here, the technique involves using sound pressure and referenced phase data on the measurement sphere to determine the spherical harmonic coefficients. Those coefficients are then used to propagate and reconstruct the sound field in either of two directions: outward, to visualize the sound field, or inward for the purpose of noise source identification. The acoustic particle velocity and radial displacement can be calculated so that their distributions over the surface of the source may be visualized. The pressure and velocity results can then be combined to yield the acoustic intensity.

THEORY

The radiation of sound from vibrating spherical bodies is described in detail by Morse and Ingard [4]. In short, the wave equation is solved in spherical coordinates by separation of variables so that the radial dependence of the sound field is described by spherical Hankel functions, and the polar and azimuthal dependence is described by the Legendre functions, through which the spherical harmonics can be calculated. The general series solution may be expressed as [4]:

$$P(M,\omega) = \sum_{n=0}^{+\infty} h_n(kr) \sum_{m=0}^{n} [A_{nm}Y^{+}_{nm}(\theta,\varphi) + B_{nm}Y^{-}_{nm}(\theta,\varphi)] \tag{1}$$

where $P(M,\omega)$ is the complex pressure at frequency ω and locations M on a spherical surface of radius r. The spherical Hankel function, $h_n(kr)$, can easily be computed using a linear combination of the spherical Bessel and Neumann functions. The spatial harmonics $Y^+_{nm}(\theta,\varphi)$ and $Y^-_{nm}(\theta,\varphi)$ are described in terms of m differentiations of the n^{th} order Legendre function expanded in powers of $\cos\theta$. A harmonic time dependence of the form $e^{j\omega t}$ is assumed, θ is the polar angle measured from the positive z-axis, and φ is the azimuthal angle measured from the positive x-axis. The harmonic coefficients A_{mn} and B_{nm} can be determined by taking advantage of the orthogonality of the spherical harmonics [2] i.e.;

$$A_{nm} = \varepsilon_m \frac{(2n+1)}{4\pi} \frac{(n-m)!}{(n+m)!} \frac{1}{h_n(kr)} \int_0^{2\pi} \int_0^{\pi} P(M,\omega) Y^+_{nm}(\theta,\varphi) sin\theta \, d\theta d\varphi$$
$$B_{nm} = \varepsilon_m \frac{(2n+1)}{4\pi} \frac{(n-m)!}{(n+m)!} \frac{1}{h_n(kr)} \int_0^{2\pi} \int_0^{\pi} P(M,\omega) Y^-_{nm}(\theta,\varphi) sin\theta \, d\theta d\varphi \qquad (2)$$

where

$$\varepsilon_m = \begin{Bmatrix} 1 & m = 0 \\ 2 & m \geq 1 \end{Bmatrix}. \qquad (3)$$

Equations (2) must be discretzed when used in combination with measured pressures. When the harmonic coefficients are known, the pressure or particle velocity fields may be propagated away from or toward the source as needed by using the expression (1). Note that the equation (1) applies only in a free-field radiation environment. Reflected components may be accounted for by using the complex conjugate of the Hankel function as explained by Weinreich and Arnold [2].

NUMERICAL SIMULATION

The performance and capabilities of the holographic algorithm were first studied through numerical simulation. A program was written to predict the pressure field at a given radius due to any number of monopole sources. The coefficients A_{nm} and B_{nm} were then estimated using discretized versions of equations (2). The resulting harmonic coefficients could then be used to reproduce the complex pressure, which may be compared to the theoretical data at any radius to check accuracy. The strengths, phases, and locations of the sources are variable so that higher order radiation patterns (e.g. dipole) may be simulated. In all cases, the "measurement sphere" had a radius of one meter.

Simple monopole and dipole cases were completed to compare with analytical calculation of the harmonic coefficients. To demonstrate convergence and the ability of the technique to handle higher order sources, a lateral quadrupole placed at the origin (in the x-y plane) was used. The sharp directivity pattern of the quadrupole provides a good test for the accuracy of the algorithm, and its harmonic coefficients are significant up to third order; i.e., A_{00}, A_{20}, and A_{22}. In figure 1, the real and imaginary parts of the exact and reconstructed complex pressure from the quadrupole are compared at a reconstruction radius of 0.5 meter. The data shown is for a meridian ($\varphi = 0$) line around the sphere, and the number of "measurement" points around the sphere in both the polar and azimuthal directions was 34. Agreement between the predicted and actual values is very good, with an error of less than 0.2 dB at all points. A match of both real and imaginary parts shows that the reconstructed magnitude and phase information is accurate. Any error is due to the discrete approximation of the integrals in equations (2).

EXPERIMENT

Holographic techniques have proven useful in the area of noise source identification. The spherical acoustic holography employed here also has potential in these applications, particularly with small machinery. To accomplish the objective of bringing the technique from simulation to experiment, we have used it to visualize the acoustic fields of an unknown noise source consisting of a shell of a refrigeration compressor excited internally by a shaker. The measurement system comprised an array of microphones which was rotated to the proper locations with a boom system. The outputs of the microphones, in volts, were measured and converted to sound pressure. In all experimental cases, measurements were made at 20 equally spaced points per complete meridian and 20 equally spaced azimuthal angles.

Refrigeration compressor shells have been the subject of many vibration studies, and one having an approximately spheroidal shape provided a convenient noise source for this technique. To simulate a compressor in operation, a one pound shaker was mounted on the internal suspension springs, as shown in figure 4, with its stinger driving the lower shell at a point near the compressor's discharge tube. The acoustic frequency spectrum at a single microphone position from a random noise input to the shaker indicated a significant peak at 600 Hz, so a sine wave at this frequency was used in the initial holographic experiment. The first measurement sphere was at a one meter radius, with a successful verification measurement at 0.5 meters.

The real power of any holographic technique is its ability to propagate the sound field back to a noise source, and to reconstruct the sound pressure, particle velocity, radial displacement, and sound intensity at the surface of the source. Observation of these fields may then allow the causes of the radiation patterns seen in the farfield to be determined. The spherical holography technique can be used to calculate these quantities quite easily. To approximate the surface of the compressor, a sphere with a radius large enough to enclose the entire shell was employed: that radius was 0.105 meters. A mesh plot (figure 3) of the radial displacement at the surface at 600 Hz illustrates that at this frequency, the compressor shell is moving back and forth as a rigid body. This plot represents the shell "unfolded" along the azimuthal and polar angles. The front side of the surface is located in the middle of the mesh, as labeled. A similar plot in figure 4 of the surface acoustic intensity locates the two areas on the shell which are radiating the most sound power.

Visualization of the reconstructed sound field at various radii in the farfield indicated a strong dipole radiation pattern (shown in figure 5), the axis of which corresponds to the axis of the driver inside the shell. This conclusion can be confirmed by inspection of the harmonic coefficients since the largest coefficient appears in the same location as that of a dipole oriented along the x-axis.

A second set of measurements, this time with broad band white noise excitation of the shell and a decreased measurement radius at 18 cm, were performed to investigate higher frequency behavior. A resonance at approximately 2372 Hz allowed the location of the shaker forcing to be "found". Figure 6 shows a large peak of acoustic intensity in the front, just below the equator of the shell. This is approximately where the shaker was mounted. This result is quite dramatic and shows that the spherical technique is capable of accomplishing the same tasks as other holographic methods.

The final objective of this work was to test machine noise generated by refrigerator compressors running under standard conditions. An initial set of testing produced data that was particularly coherent in the lower frequency ranges, so these frequencies were investigated. Traditionally, the acoustic gas cavity resonances of a hermetic compressor are located in this range. The holographic technique allowed the visualization of the surface mode shapes that result from these resonances. In figure 7, the variation of the mode shape with frequency is demonstrated for a single compressor. Figure 8 shows that the modal pattern at 400 Hz did not vary significantly when aspects of the compressor's internal configuration was altered.

CONCLUSIONS

Previous work has expanded the family of holographic techniques to include spherical holography. The present work applied the method in both simulation and experiment. The ultimate goal of application to noise source identification was shown to be feasible through a test on a compressor shell, and tests of compressors running under thermal loading. Insight gained into the vibration patterns of the surface of the shell in the shaker experiment accounted for the sound radiation patterns in the farfield, and the location of the shaker forcing was found using the acoustic intensity at higher frequencies. In application to the running compressor, the shell's modal patterns resulting from gas cavity resonances were visualized. The results allow an insight to be gained into the location and motion of internal mechanisms that are causing the patterns, and to see how changes to the design may affect these patterns. The technique has been shown to be useful in its current form. However, a measurement system with the capability to accurately take sound pressure data at a large number of locations simultaneously would greatly enhance the power of the method, allowing "real time holograms" to be obtained at various times during the machine's operation.

ACKNOWLEDGMENTS

The authors would like to thank Americold, Inc. for their financial support of this work and J. Wood of the Herrick Labs shop for his technical assistance.

REFERENCES

[1] "Nearfield Acoustical Holography: I. Theory of Generalized Holography and the Development of NAH", J.D. Maynard, E.G. Williams and Y. Lee, J. Acoust. Soc. Am., **74**, 1395-1413 (1985)

[2] "Method for Measuring Acoustic Radiation Fields", G. Weinreich and B. Arnold, J. Acoust. Soc. Am., **68**, 404-411, (1980).

[3] "Spherical Acoustical Holography Using Sound Intensity Measurements: Theory and Simulation," F. Laville, M. Sidki, J. Nicolas, Acustica, **76**, 193-198 (1992).

[4] Morse, P.M., Ingard, K.U., Theoretical Acoustics. McGraw-Hill, New York, 1968

[5] "Generalized Nearfield Acoustical Holography for Cylindrical Geometry: Theory and Experiment', E. Williams and H. Dardy, J. Acoust. Soc. Am., **81**, 389-407, (1987).

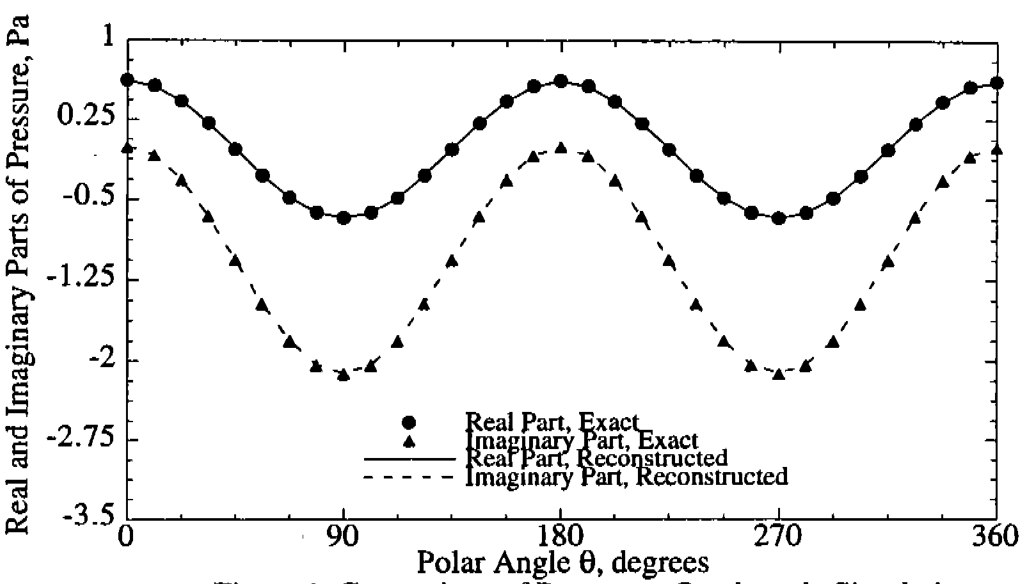

Figure 1. Comparison of Pressures, Quadrupole Simulation

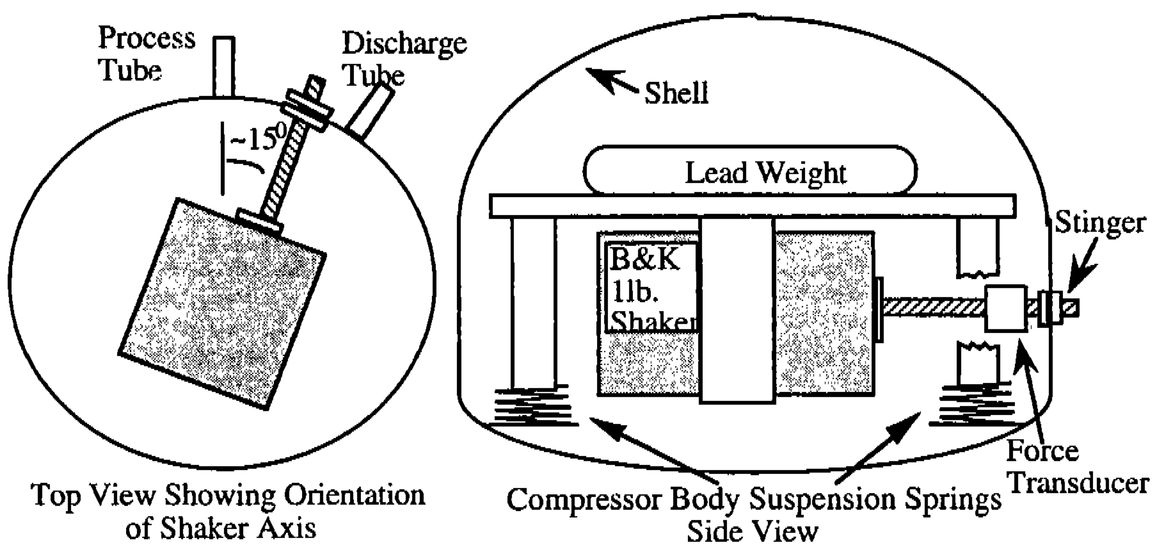

Figure 2. Experimental Set Up For Excitation of Compressor Shell

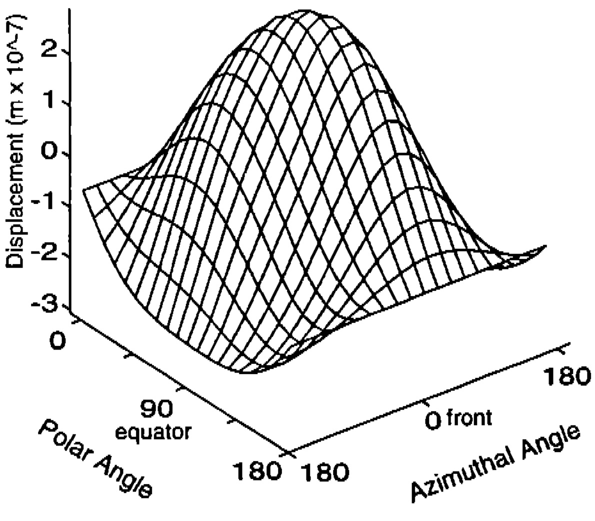

Figure 3. Radial Displacement at Shell Surface, Shaker Experiment, 600 Hz

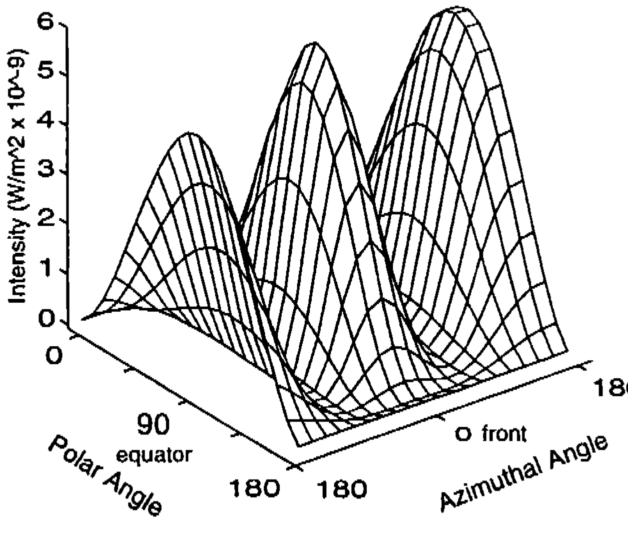

Figure 4. Acoustic Intensity at Shell Surface, Shaker Experiment, 600 Hz

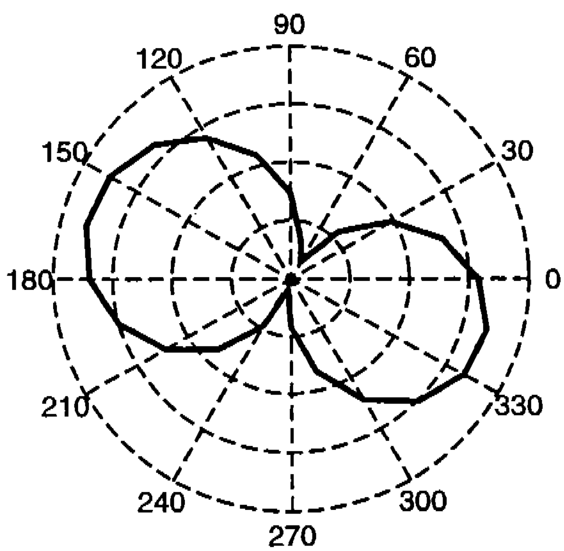

Figure 5. Directivity Pattern Around Equator at 1 meter, Shaker Experiment, 600 Hz

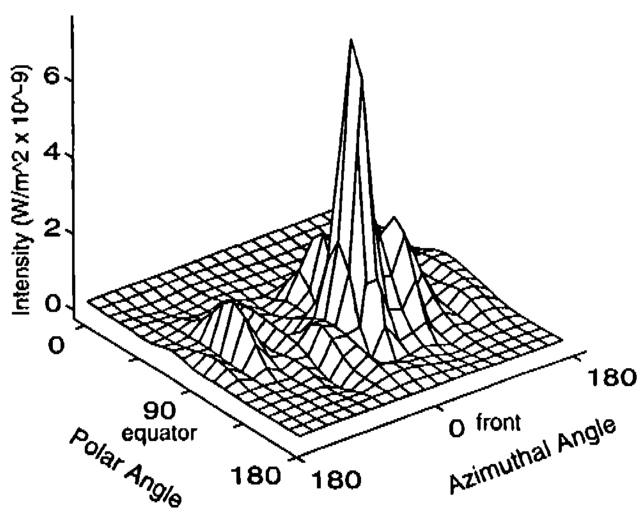

Figure 6. Acoustic Intensity at Shell Surface, Shaker Experiment, 2372 Hz

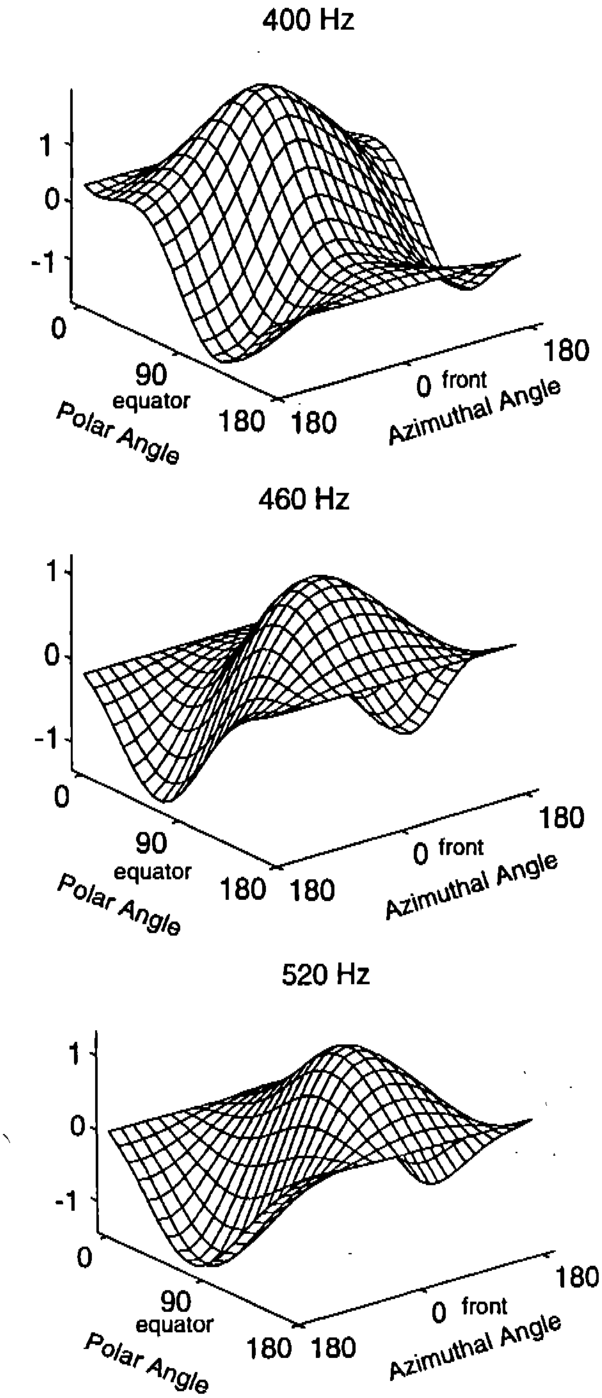

Figure 7. Comparison of Normalized Sound Pressure Mode Shapes Over Frequency, Running Compressor Experiment

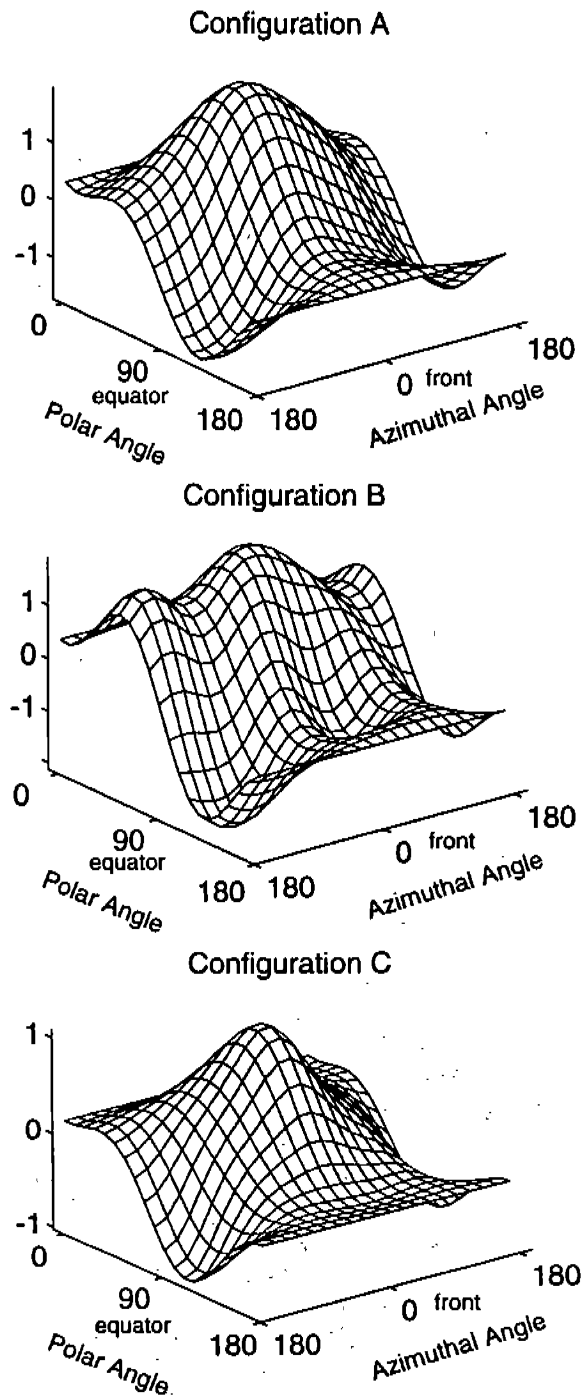

Figure 8. Comparison of Normalized Sound Pressure Mode Shapes Over Compressor Configuration, Running Compressor Experiment